

Iron(II,III)–Polyphenol Complex Nanoparticles Derived from Green Tea with Remarkable Ecotoxicological Impact

Zdenka Markova,[†] Petr Novak,[†] Josef Kaslik,[†] Pavla Plachtova,^{‡,§} Marketa Brazdova,^{‡,§} Daniel Jancula,[‡] Karolina Machalova Siskova,[†] Libor Machala,[†] Blahos Marsalek,^{‡,§} Radek Zboril,^{*,†} and Rajender Varma^{*,||}

[†]Regional Centre of Advanced Technologies and Materials, Departments of Physical Chemistry and Experimental Physics, Faculty of Science, Palacky University in Olomouc, Slechtitelu 11, 78371 Olomouc, Czech Republic

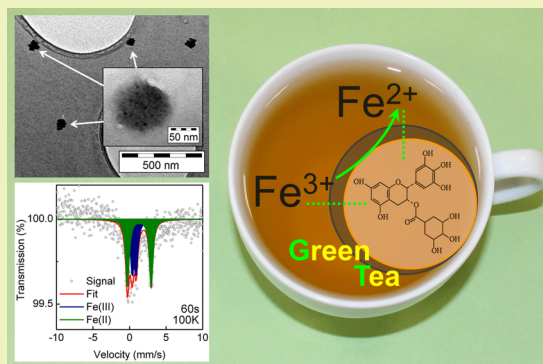
[‡]Institute of Botany, Academy of Sciences of the Czech Republic, Lidicka 25/27, 60200 Brno, Czech Republic

[§]Research Centre for Toxic Compounds in the Environment (RECETOX), Faculty of Science, Masaryk University, Kamenice 753/5, Building A29, 62500 Brno, Czech Republic

^{||}Sustainable Technology Division, National Risk Management Research Laboratory, U.S. Environmental Protection Agency, 26 West Martin Luther King Drive, MS 443, Cincinnati, Ohio 45268, United States

ABSTRACT: There are several green methods available to synthesize iron-based nanoparticles using different bio-based reducing agents. Although their useful properties in degradation of organic dyes, chlorinated organics, or arsenic have been described earlier, their characterization has been ambiguous, and further research is needed in this area. Synthesis and characterization details on iron-based nanoparticles produced by green tea extract are described in detail; characterization was carried out by transmission electron microscopy (TEM), X-ray powder diffraction (XRD), and UV–vis spectrometry followed by ecotoxicological assay. XRD and TEM analyses revealed that iron forms amorphous nanosized particles with size depending on reaction time. Moreover, low-temperature Mössbauer spectroscopy confirmed progressive reduction of Fe³⁺ to Fe²⁺ during the reaction. Finally, the iron(II,III) nanoparticles prepared by green tea extract (GT–Fe nanoparticles) were found to have negative ecotoxicological impacts on important aquatic organisms such as cyanobacterium (*Synechococcus nidulans*), alga (*Pseudokirchneriella subcapitata*), and even invertebrate organisms (*Daphnia magna*). The EC₅₀ values are 6.1 ± 0.5 (72 h), 7.4 ± 1.6 (72 h), and 21.9 ± 4.3 (24 h) mg of Fe per L, respectively.

KEYWORDS: Green synthesis, Green tea polyphenols, Iron-complexed nanoparticles, Ecotoxicity, Mössbauer spectroscopy



INTRODUCTION

The environmentally friendly greener processes in chemistry and chemical technology are becoming increasingly popular as a result of worldwide problems associated with environmental contamination.¹ The techniques for obtaining nanomaterials using naturally occurring reagents such as plant extracts, vitamins, polymers, or microorganisms as reducing and stabilizing agents are garnering attention in nanotechnology. These syntheses have led to the fabrication of several inorganic nanoparticulate systems, including silver,^{2,3} gold,⁴ copper,⁵ and palladium,³ among others.¹

Among the nanoparticles mentioned above, iron-based materials (i.e., zero-valent iron nanoparticles, iron oxides, and hydroxides nanoparticles) are of significant interest because of their efficiency in the remediation of pollutants from soils and disinfection of water. Among these materials, zero-valent iron nanoparticles (nZVI) have found widespread use because of their cost-effective and relatively environmentally friendly nature.^{6–10} Recent studies have shown that nZVI particles

enable reduction, sorption, and/or both processes simultaneously when applied against a broad range of common environmental contaminants.^{8,9} Several methods have been used for the production of these nanoparticles including the decomposition of iron pentacarbonyl (Fe(CO)₅) in organic solvents,¹¹ reduction of Fe²⁺ or Fe³⁺ to nZVI with sodium borohydride¹² or ethylene glycol,¹³ or the process of breaking large bulk materials into smaller nanoparticles such as with the ball milling method.¹⁴ However, these methods present several limitations and formidable problems, such as the use of hazardous reducing agents or precursors and agglomeration of nanoparticles that leads to formation of larger aggregates due to van der Waals and magnetic forces. Bio-based methods might

Special Issue: Sustainable Nanotechnology 2013

Received: February 27, 2014

Revised: April 8, 2014

Published: April 21, 2014

be more appropriate options for designing nanomaterials with diminution of environmental impacts. Consequently, “greener” synthetic methods using mainly tea, fruit, or plant extracts containing antioxidants based on polyphenols have been utilized for generating Fe-containing nanoparticles and their environmental remediation applications.^{15–23} Moreover, the use of plants for the synthesis of nanoparticles could be advantageous over the conventional chemical methodologies because plants are biorenewable resources and can possibly provide sustainable solutions for large-scale deployment. The tea polyphenols are often the prime choice for reducing and stabilizing agents because polyphenols are biodegradable, nontoxic, and water-soluble at room temperature. Moreover, tea extract contains molecules bearing alcoholic functional groups that can be exploited for stabilization of the prepared material; tea polyphenols can also form complexes with iron ions and thereafter reduce them to metal nanoparticles.¹⁸ In this context, oxidation/reduction processes in the reaction depend on the reduction potentials (E^0) of reagents. While the reduction potential values for tea or fruit polyphenols range between 0.3 and 0.8 V,^{18,20} the reduction potential of Fe metal is strongly negative (-0.44 V). Therefore, the tea and fruit polyphenols themselves are unsuitable for the reduction of Fe^{3+} and Fe^{2+} ions to zero-valent iron and only polyphenol-assisted reduction of Fe^{3+} to Fe^{2+} is possible (reduction potential of $\text{Fe}^{3+}/\text{Fe}^{2+}$ is 0.771 V) as well as polyphenol-assisted reduction of silver ($E^0 [\text{Ag}^+/\text{Ag}] = 0.799$ V), gold ($E^0 [\text{Au}^{3+}/\text{Au}] = 1.498$ V), or palladium ($E^0 [\text{Pd}^{2+}/\text{Pd}] = 0.987$ V) ions to their respective metal nanoparticles.

Although several studies have been conducted on the use of bio-based materials for synthesis of nZVI, further research is needed in this area in view of the ambiguous conclusions. The previously prepared Fe-based nanoparticles using green chemistry were identified as amorphous nZVI using transmission electron microscopy (TEM) and X-ray powder diffraction (XRD).^{15,16,18,19,21} On the contrary, the recent studies reveal that iron is not reduced to nZVI by polyphenols but probably forms an iron(III)–polyphenol complex (determined by energy dispersive spectrophotometry).²² Nevertheless, these methods are unable to determine the phase composition of the amorphous iron-containing material. Therefore, in this paper, we have synthesized green tea–iron nanoparticles (GT–Fe) and characterized them by several analytical methods including TEM, XRD, UV–vis spectroscopy, and Mössbauer spectroscopy. Mössbauer spectroscopy, in particular, presents one of the most powerful tools in identification of both crystalline and amorphous iron-containing phases.^{24–27} Control experiments have been conducted using the standard borohydride reduction method leading to a synthesis of nZVI, and the results were compared with the greener approach. In view of earlier successful remediation studies with these GT–Fe nanomaterials in degradation of organic dyes,^{15,16,22} chlorinated organics,¹⁷ arsenic(III),²³ or in the catalytic chemoselective dehydrogenation reactions,²⁹ the correct identification of their composition and their ecotoxicological studies have been carried out and discussed because their use in wastewater remediation places them in direct contact with the environment.

EXPERIMENTAL SECTION

Materials and Chemicals. Iron(III) chloride hexahydrate ($\text{FeCl}_3 \cdot 6\text{H}_2\text{O}$), iron(III) nitrate nonahydrate ($\text{Fe}(\text{NO}_3)_3 \cdot 9\text{H}_2\text{O}$), and sodium borohydride (NaBH_4) were purchased from Sigma-Aldrich. Tea

extract was prepared from green tea leaves purchased from a local market. All chemicals were used without further purification.

Biosynthesis of Fe-Based Nanoparticles. The synthesis of iron-based nanoparticles using green tea extract (GT–Fe) was performed according to the protocol described by Nadagouda et al.,¹⁸ with a minor modification that consists of maintaining the reaction under nitrogen atmosphere. Briefly, tea extract was prepared by adding 2.0 g of tea powder to 100 mL hot water (just after boiling). The extract was allowed to cool to room temperature under magnetic stirring and was vacuum filtered. Separately, the solution of 0.1 M $\text{Fe}(\text{NO}_3)_3 \cdot 9\text{H}_2\text{O}$ was prepared, and both solutions were bubbled with nitrogen gas for 1 h. Subsequently, green tea-synthesized Fe-based nanoparticles were prepared by injecting 0.5 M $\text{Fe}(\text{NO}_3)_3 \cdot 9\text{H}_2\text{O}$ into green tea extract in a 1:5 volume ratio under nitrogen atmosphere. The reaction was continued for 24 h, and the product was stored at 4 °C. A control authentic sample of nZVI was prepared via a standard NaBH_4 reduction method.¹²

Material Characterization. Morphological and size characteristics were analyzed using transmission electron microscopy (TEM). TEM images were obtained using an electron microscope JEOL JEM-2010 operating at 160 kV with a point-to-point resolution of 1.9 Å. For all measurements, a drop of a very dilute dispersion was placed on the copper grid with holey carbon film and subsequently allowed to dry under vacuum at room temperature (RT).

X-ray powder diffraction (XRD) patterns of Fe-based samples were recorded on PANalytical X'Pert PRO diffractometer in Bragg–Brentano geometry, equipped with an iron-filtered CoK_α radiation source ($\lambda = 0.179$ nm) at 40 kV/30 mA, X'Celerator detector, programmable divergence, and diffracted beam anti-scatter slits. Generally, 200 μL of suspension was dropped on a zero-background single-crystal Si slide, allowed to dry under vacuum at RT, and scanned in continuous mode (resolution of $0.017^\circ 2\theta$, scan speed of $0.008^\circ 2\theta$ per second, 2θ range from 20° to 105°) under ambient conditions. The commercially available standards SRM640 (Si) and SRM660 (LaB6) from NIST were used for the evaluation of line positions and instrumental line broadening, respectively. The acquired patterns were processed using X'Pert HighScore Plus software (PANalytical, The Netherlands), in combination with PDF-4+ and ICSD databases (ICSD collection code for α -Fe is 631729).

Absorbance was measured at wavelengths ranging between 200 and 900 nm at RT using a Lightwave II (WPA) UV–vis spectrophotometer. For all measurements, the samples were appropriately diluted with ddH_2O .

A transmission Mössbauer spectrometer MS96²⁸ with a $^{57}\text{Co}(\text{Rh})$ source of γ -rays was used for the zero-field Mössbauer experiment at 100 K. The obtained spectra were fitted by the Lorentzian line shapes using program MossWinn³⁰ based on the least-squares method. The isomer shift values were referred to α -Fe foil sample at room temperature. For all measurements, the reaction was stopped at 1 min, 60 min, and 24 h by an anaerobic injection of 200 μL of the sample into pre-frozen (liquid nitrogen) Mössbauer cuvettes. The samples were then immediately stored at -80°C to protect against possible oxidation.

The iron content was determined due to the reaction of ferrozine (monosodium salt hydrate of 3-(2-pyridyl)-5,6-diphenyl-1,2,4-triazine-*p,p'*-disulfonic acid)²⁴ and the divalent Fe form, where a stable magenta complex is formed. In order to determine the iron concentration in the samples, bMNPs were separated by centrifugation, resuspended in 65% (w/w) HNO_3 , and incubated at 98°C for 1 h to dissolve the MNPs. The iron content in the solution was determined with a protocol of the ferrozine assay described by Viollier.³¹

Ecotoxicological Bioassay. For all bioassays, aqueous dispersion of GT–Fe nanoparticles was added to the cultivation media to achieve various final concentrations (see below) expressed as mg/L of Fe.

Pseudokirchneriella subcapitata and *Synechococcus nidulans*. The growth assays with the green alga *P. subcapitata* and cyanobacterium *S. nidulans* were performed in 96-well microplates with a sample volume of 250 μL per well with three replicates for each sample. The initial concentration was 50,000 cells per milliliter and

200,000 cells per milliliter for alga and cyanobacterium, respectively. For the tests, ZBB growth medium, i.e., a 1:1 mixture of medium Z (Zehnder)³² and Bold's Basal medium (BB)^{33,34} was used. Algae were exposed to the material for 72 h at 24(±1) °C under continuous illumination (90 μmol/m² s) by cool white fluorescent lamps (Philips). The growth was evaluated after 72 h by *in vivo* fluorescence measurements with a microplate fluorescence reader GENios (Tecan). Inhibition of growth in different concentrations of chemicals was used as the end point while determining the EC₅₀.

Daphnia magna. *D. magna* bioassays were performed according to the international standard method (ISO 6341, 1996).³⁵ Organisms were obtained from RECETOX (Masaryk University, Brno, Czech Republic). Juveniles of *D. magna* (20 individuals per variant, not older than 24 h) were transferred into separate polystyrene plates using the standard exposure solution ISO 6341. The temperature was kept at 20(±2) °C during the exposure. Daphnids were inspected after 24 and 48 h of exposure. The toxicity of material was expressed in terms of the effective concentration (EC₅₀) required to cause the immobilization of 50% of all individuals after 24 and 48 h of interaction.

RESULTS AND DISCUSSION

Characterization. On adding ferric chloride solution to the aqueous extract of green tea leaves under nitrogen atmosphere, the mixture instantaneously turned from a yellow–orange to dark brown–black color (Figure 1) indicating the formation of

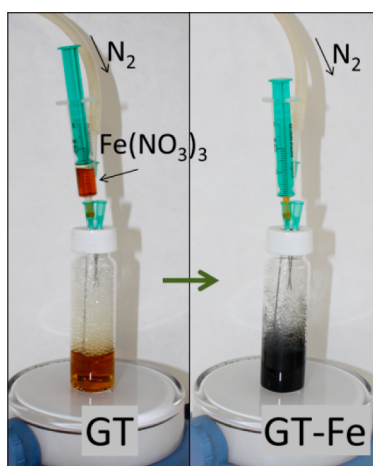


Figure 1. Photographic images of color development during formation of the GT–Fe complex before mixing GT and Fe salt (left) and after mixing (right) in the synthesis GT–Fe nanoparticles.

green tea–iron complex (GT–Fe), as described recently.²² The reaction was carried out for 24 h, and 1 mL of the sample was taken out (using anaerobic sampling by injection) at 1 min, 60 min, and 24 h for further analysis. As a control, nZVI particles were prepared by the standard borohydride reduction method, and the sample was labeled as BH–Fe.

UV–vis spectra of GT–Fe nanoparticles, green tea (GT), BH–Fe, and Fe(NO₃)₃·9H₂O are shown in Figure 2. The spectra for all samples in the visible range have continuous absorption. On the other hand, two significant absorption peaks in the UV range were observed in the spectra of GT and GT–Fe, and Fe(NO₃)₃·9H₂O, while these peaks were not present in the spectrum of BH–Fe (no surface plasmon resonance absorption was observed in whole spectrum). The absorption peak at 210–220 nm is identical for all samples (except BH–Fe). The second peak of the spectra ranging between 250 and 400 nm is more interesting because its absorption maximum shifts from 267 to 295 nm when spectra of samples are

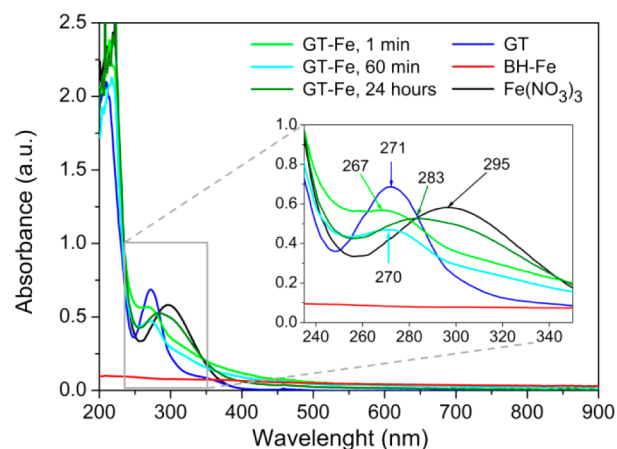


Figure 2. UV–vis spectra of GT–Fe nanoparticles taken at 1 min, 60 min, and 24 h of reaction time: green tea (GT), BH–Fe, and Fe(NO₃)₃·9H₂O, respectively.

compared. The precursors, green tea and iron(III) nitrate, have absorption peaks at 271 and 295 nm, respectively. There is a formation of complex between iron ions and polyphenols (green tea extract) just after mixing the compounds that leads to the absence of the peak at 295 nm and the peak belonging to GT shifts from 271 to 267 nm in the spectrum of GT–Fe at 1 min of the reaction. This complex changes as the reaction time progressed because the peak maximum shifts to the higher wavelengths, i.e., to 270 and 283 nm at 60 min and 24 h, respectively. This aging of the GT–Fe complex will be discussed later with the respective Mössbauer spectroscopy results.

Morphology and size of GT–Fe nanoparticles were analyzed by transmission electron microscopy (Figure 3). The recorded TEM micrographs of the GT–Fe samples taken at different time points indicate morphology development of nanomaterial structures in specified moments of the reaction. Whereas GT–Fe forms 70 nm-sized separated spherical nanoaggregates after 1 min of the reaction (Figure 3a), after 1 h, it forms larger irregular nanoparticulate structures (Figure 3b), which after 24 h turned into an extended network (Figure 3c). These morphological differences could be attributed to reaction time and/or the concentration of polyphenols in the reaction because similar structures were described previously by Wang et al.²²

XRD patterns of GT–Fe and BH–Fe nanoparticles are shown in Figure 4. The BH–Fe nanoparticles are identified as crystalline zero-valent iron nanoparticles in agreement with reported values (JCPDS card no. 04-002-685), and their mean X-ray diffraction coherence lengths (MLC) calculated from Rietveld refinement is equal to 13 nm. On the other hand, the patterns of the three GT–Fe samples lack distinct diffraction lines, suggesting that the GT–Fe NPs are amorphous in nature.^{15,18,19,22,36} In this context, amorphous XRD patterns have been interpreted differently by the authors. Wang et al.²¹ identified two very wide peaks at positions 20–25° and 40–45° 2θ Cu Kα. Their broad shapes, described as shoulders, were attributed to organic matter and α-Fe, respectively. Nevertheless, only the amorphous nature of the material can be concluded by XRD due to the lack of other diffraction lines that would enable identification of nZVI or other crystalline phases. On the other hand, Hoag et al.³⁶ prepared and identified crystalline iron nanoparticles (JCPDS card no. 00-050-1275).

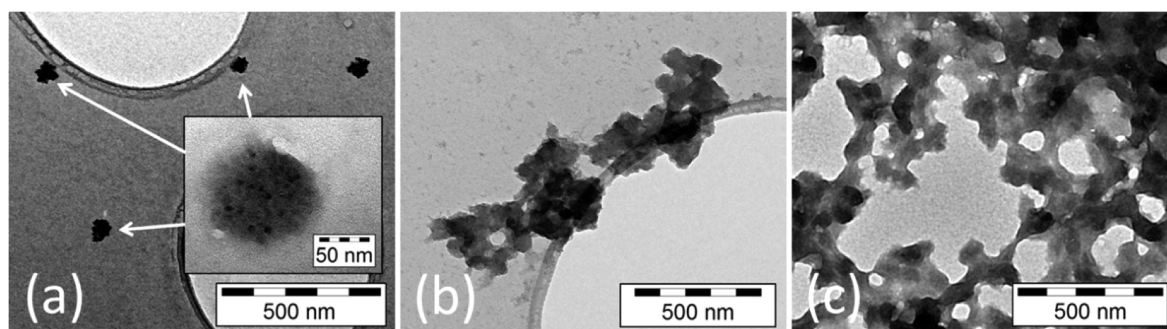


Figure 3. Morphologies of GT–Fe determined by TEM: (a) GT–Fe nanoparticles taken at (a) 1 min, (b) 60 min, and (c) 24 h of reaction time.

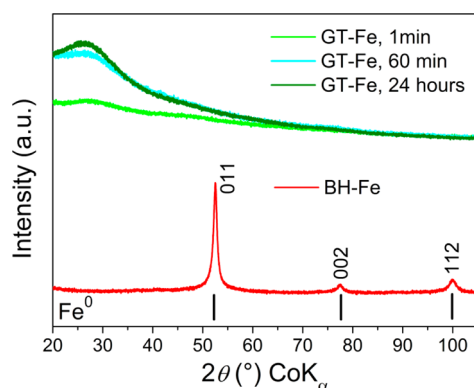


Figure 4. XRD patterns of GT–Fe taken at 1 min, 60 min, and 24 h of reaction time and BH-Fe.

Although the identified JCPDS card belongs to hexagonal zero-valent iron, this structure of iron is very improbable under

ambient conditions, and its stability at room temperature was predicted only at pressures higher than 13 GPa.³⁷

Low-temperature (100 K) Mössbauer spectroscopy is now used to determine the oxidation state of iron during its reaction with GT extracts. Mössbauer spectra of GT–Fe samples (Figure 5a–c) consist of two doublets with hyperfine parameters typical for high-spin Fe^{2+} ($\delta = 1.34$ mm/s, $\Delta E_Q = 3.25$ mm/s) and high-spin Fe^{3+} ($\delta = 0.63$ mm/s, $\Delta E_Q = 0.56$ mm/s). The presence of the both Fe^{2+} and Fe^{3+} in GT–Fe nanoparticles is in a good agreement with the above predicted reduction of Fe^{3+} to Fe^{2+} ($E^0 [\text{Fe}^{3+}/\text{Fe}^{2+}] = 0.987$ V) by GT polyphenols ($E^0 [\text{polyphenols}] \sim 0.3\text{--}0.8$ V). Moreover, the $\text{Fe}^{3+}/\text{Fe}^{2+}$ ratio was found to depend on reaction time (quantitative data are shown in Table 1). The percentage distribution of Fe^{3+} and Fe^{2+} ions in GT–Fe is calculated to be 41% and 59%, respectively, after 1 min of reaction (Figure 5a). Ongoing reduction of Fe^{3+} by GT resulted in composition of 33% Fe^{3+} and 67% Fe^{2+} at 60 min of reaction (Figure 5b), and finally 27% Fe^{3+} and 73% Fe^{2+} at 24 h of reaction (Figure 5c). Furthermore, it should be noted that no zero-valent iron

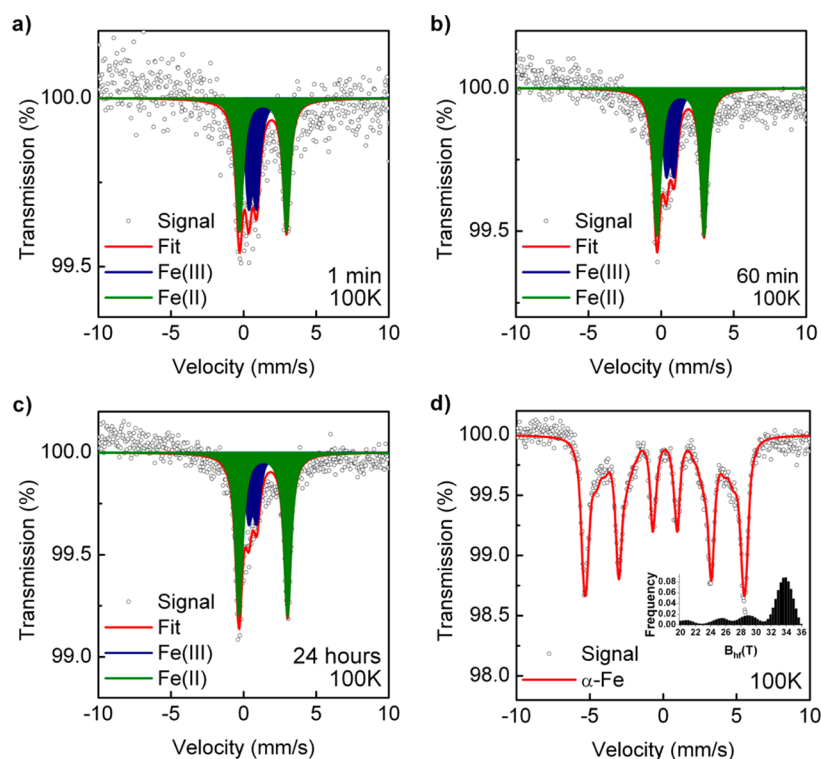


Figure 5. Low-temperature Mössbauer spectra of GT–Fe taken at (a) 1 min, (b) 60 min, and (c) 24 h of reaction time and (d) BH–Fe.

Table 1. Mössbauer Hyperfine Parameters Derived from Low-Temperature (100 K) Mössbauer Spectra^a

sample	component	$\delta \pm 0.01$ (mm/s)	$\Delta E_Q \pm 0.01$ (mm/s)	$B_{\text{hf}} \pm 0.3$ (T)	$\Gamma \pm 0.01$ (mm/s)	RA ± 1 (%)	assignment
1 min	doublet	1.34	3.25	—	0.58	59	Fe(III)
	doublet	0.63	0.56	—	0.58	41	Fe(II)
60 min	doublet	1.34	3.25	—	0.58	33	Fe(III)
	doublet	0.63	0.56	—	0.58	67	Fe(II)
24 h	doublet	1.34	3.25	—	0.58	27	Fe(III)
	doublet	0.63	0.56	—	0.58	73	Fe(II)
α -Fe	sextet	0.11	-0.01	32	0.38	100	α -Fe

^a δ is isomer shift, ΔE_Q is quadrupole splitting, B_{hf} is hyperfine magnetic field, Γ is spectral line width (determined as full width at half-maximum), and RA is the relative subspectrum area expressing atomic % of Fe (Lamb-Mössbauer f-factor is considered to be the same for all identified phases).

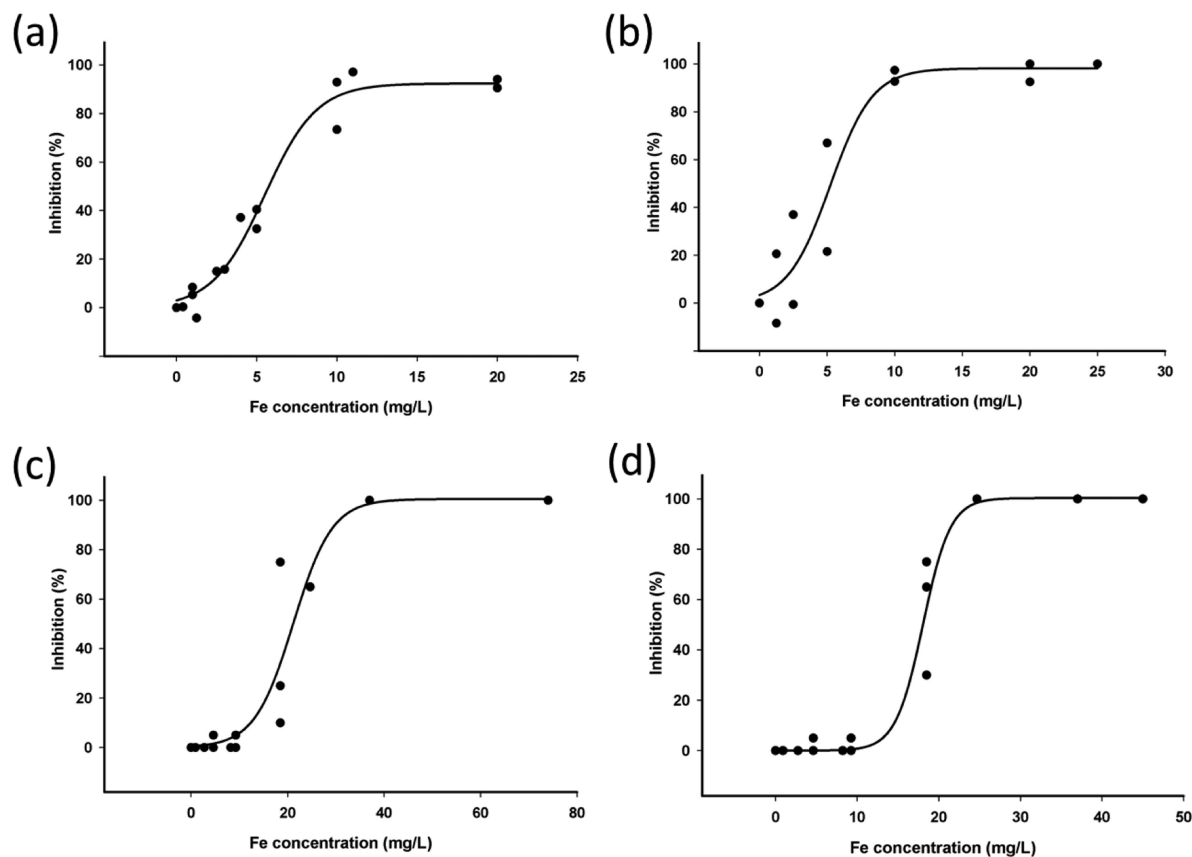


Figure 6. Ecotoxicological bioassays indicate a high activity of GT-Fe nanoparticles against (a) *S. nidulans* (after 72 h), (b) *P. subcapitata* (after 72 h), and *D. magna* after (c) 24 h and (d) 48 h.

existence has been proven after comparison of the Mössbauer spectra of GT-Fe nanoparticles with the spectrum of BH-Fe where a pure zero-valent iron is identified through the sextet component (Figure 5d).

Ecotoxicological Bioassay. As we have now uncovered the true nature of GT-Fe nanoparticles, which is different from nZVI, and because of their earlier successful remediation application that used GT-Fe nanomaterials in degradation of organic dyes,^{15,16,22} chlorinated organics,¹⁷ or arsenic(III),²³ and or in catalytic dehydrogenation reactions,²⁹ we sought to determine their impact on several organisms that can have positive or negative ecotoxicological properties. The results of a toxicological assay (Figure 6) show the negative impact of GT-Fe nanoparticles on cyanobacterium (*S. nidulans*), green alga (*P. subcapitata*), and even an aquatic invertebrate (*D. magna*). To refine, the effective GT-Fe concentrations required to inhibit 50% of organisms (EC_{50}) determined for *S. nidulans* and *P. subcapitata* were found to be 6.1 ± 0.5 and 7.4 ± 1.6 mg/L,

respectively. In addition, EC_{50} values of GT-Fe toward *D. magna* after 24 and 48 h were determined to be 21.9 ± 4.3 and 16.6 ± 4.7 mg/L, respectively.

These results can be compared with the nZVI acute toxicity results by Maršálek et al.;³⁸ the EC_{50} value for cyanobacterium *Microcystis aeruginosa* was reported to be 50 mg/L in natural conditions, which is almost 10 times lower in toxicity than the one determined for cyanobacteria when GT-Fe nanoparticles were tested (EC_{50} (*S. nidulans*) = 6.1 mg/L). Moreover, a very high toxicity of GT-Fe against other organisms (alga and invertebrate) was revealed, whereas EC_{50} values of nZVI for analogous organisms were greater than 1000 mg/L. Comparing those studies, GT-Fe can be presented as slightly-moderately toxic, while nZVI is practically “non-toxic” for the above-mentioned aquatic organisms. The significant toxicity of GT-Fe nanoparticles can be caused by the high content of Fe^{2+} ions that are probably released from GT polyphenols and may act as electron donors under aerobic conditions. Thus, Fe^{2+} can

readily catalyze the generation of noxious radicals that resulted in oxidative stress, generation of reactive oxygen intermediates, disruption of the membrane integrity, or inhibited intracellular redox processes.^{39,40} Moreover, aggregation of GT–Fe in fresh water is expected to be slower than aggregation of nZVI in the same conditions. Thus, long-term bioavailability (and thus ecotoxicity) of GT–Fe is expected to be higher when compared to the nanoparticles of zero-valent iron.

CONCLUSIONS

The detailed characterization and determination of ecotoxicological impact of green tea–iron nanoparticles has been accomplished. The reaction between polyphenols (green tea) and Fe³⁺ ions resulted in both the formation of an Fe–polyphenol nanosized complex and reduction (reaction time dependent) of Fe³⁺ to Fe²⁺, respectively. The GT–Fe nanoparticles have been assessed with ecotoxicological assays that proved their highly negative effects on three representative aquatic organisms, including cyanobacterium (*S. nidulans*), alga (*P. subcapitata*), and even invertebrate (*D. magna*). The toxicity of tested GT–Fe nanoparticles can be attributed to Fe²⁺ ions released from GT polyphenols that may act as electron donors under aerobic conditions and readily catalyze the generation of toxic noxious radicals; they should be considered in the use of these materials in remediation processes where aquatic organisms are present.

AUTHOR INFORMATION

Corresponding Authors

*Tel.: +420585634947. Fax: +420585634761. E-mail: radek.zboril@upol.cz (R.Z.).

*Tel.: +1 (513) 487-2701. Fax: +1(513) 569-7677. E-mail: Varma.Rajender@epa.gov (R.V.).

Author Contributions

All authors have given approval to the final version of the manuscript.

Notes

The authors declare no competing financial interest.

ACKNOWLEDGMENTS

The authors gratefully acknowledge the financial support by the Operational Program Research and Development for Innovations–European Regional Development Fund (project CZ.1.05/2.1.00/03.0058 of the Ministry of Education, Youth and Sports of the Czech Republic), Operational Program Education for Competitiveness – European Social Fund (projects CZ.1.07/2.3.00/20.0155 and CZ.1.07/2.3.00/20.0058), and Internal Student Grant IGA of Palacký University in Olomouc (PrF_2013_014). This research was also supported by the Czech Ministry of Education (LO1214) and the long-term research development project no. RVO 67985939 (Academy of Sciences of the Czech Republic)

ABBREVIATIONS

GT, green tea; GT–Fe, BH–Fe, borohydride zero-valent iron, green tea–iron nanoparticles; nZVI, zero-valent iron nanoparticles; TEM, transmission electron microscopy; XRD, X-ray powder diffraction; E⁰, reduction potentials

REFERENCES

- (1) Kharissova, O. V.; Dias, H. V. R.; Kharisov, B. I.; Pérez, B. O.; Pérez, V. M. J. The greener synthesis of nanoparticles. *Trends Biotechnol.* **2013**, *31*, 240–248.
- (2) Venkatpurwar, V.; Pokharkar, V. Green synthesis of silver nanoparticles using marine polysaccharide: Study of in-vitro antibacterial activity. *Mater. Lett.* **2011**, *65*, 999–1002.
- (3) Nadagouda, M. N.; Varma, R. S. Green synthesis of silver and palladium nanoparticles at room temperature using coffee and tea extract. *Green Chem.* **2008**, *10*, 859–862.
- (4) Afzal, A. B.; Akhtar, M. J.; Nadeem, M.; Hassan, M. M. Investigation of structural and electrical properties of polyaniline/gold nanocomposites. *J. Phys. Chem. C* **2009**, *113*, 17560–17565.
- (5) Xiong, J.; Wang, Y.; Xue, Q.; Wu, X. Synthesis of highly stable dispersions of nanosized copper particles using l-ascorbic acid. *Green Chem.* **2011**, *13*, 900–904.
- (6) Grieger, K. D.; Fjordbøge, A.; Hartmann, N. B.; Eriksson, E.; Bjerg, P. L.; Baun, A. Environmental benefits and risks of zero-valent iron nanoparticles (nZVI) for in situ remediation: Risk mitigation or trade-off? *J. Contam. Hydrol.* **2010**, *118*, 165–183.
- (7) Karn, B.; Kuiken, T.; Otto, M. Nanotechnology and in situ remediation: A review of the benefits and potential risks. *Environ. Health Perspect.* **2009**, *117*, 1813–1831.
- (8) Noubactep, C.; Caré, S.; Crane, R. Nanoscale metallic iron for environmental remediation: prospects and limitations. *Water, Air, Soil Pollut.* **2012**, *223*, 1363–1382.
- (9) Zhang, L.; Fang, M. Nanomaterials in pollution trace detection and environmental improvement. *Nano Today* **2010**, *5*, 128–142.
- (10) Zhang, W. Nanoscale iron particles for environmental remediation: An overview. *J. Nanopart. Res.* **2003**, *5*, 323–332.
- (11) Karlsson, M. N.; Deppert, K.; Wacaser, B.; Karlsson, L. S.; Malm, J.-O. Size-controlled nanoparticles by thermal cracking of iron pentacarbonyl. *Appl. Phys. A: Mater. Sci. Process.* **2004**, *80*, 1579–1583.
- (12) Sun, Y.-P.; Li, X.; Cao, J.; Zhang, W.; Wang, H. P. Characterization of zero-valent iron nanoparticles. *Adv. Colloid Interface Sci.* **2006**, *120*, 47–56.
- (13) Valle-Orta, M.; Diaz, D.; Santiago-Jacinto, P.; Vázquez-Olmos, A.; Reguera, E. Instantaneous synthesis of stable zerovalent metal nanoparticles under standard reaction conditions. *J. Phys. Chem. B* **2008**, *112*, 14427–14434.
- (14) Li, S.; Yan, W.; Zhang, W. Solvent-free production of nanoscale zero-valent iron (nZVI) with precision milling. *Green Chem.* **2009**, *11*, 1618–1626.
- (15) Njagi, E. C.; Huang, H.; Stafford, L.; Genuino, H.; Galindo, H. M.; Collins, J. B.; Hoag, G. E.; Suib, S. L. Biosynthesis of iron and silver nanoparticles at room temperature using aqueous sorghum bran extracts. *Langmuir* **2011**, *27*, 264–271.
- (16) Shahwan, T.; Abu Sirriah, S.; Nairat, M.; Boyacı, E.; Eroğlu, A. E.; Scott, T. B.; Hallam, K. R. Green synthesis of iron nanoparticles and their application as a Fenton-like catalyst for the degradation of aqueous cationic and anionic dyes. *Chem. Eng. J.* **2011**, *172*, 258–266.
- (17) Smuleac, V.; Varma, R.; Sikdar, S.; Bhattacharyya, D. Green synthesis of Fe and Fe/Pd bimetallic nanoparticles in membranes for reductive degradation of chlorinated organics. *J. Membr. Sci.* **2011**, *379*, 131–137.
- (18) Nadagouda, M. N.; Castle, A. B.; Murdock, R. C.; Hussain, S. M.; Varma, R. S. In vitro biocompatibility of nanoscale zerovalent iron particles (NZVI) synthesized using tea polyphenols. *Green Chem.* **2010**, *12*, 114–122.
- (19) Machado, S.; Pinto, S. L.; Grosso, J. P.; Nouws, H. P.; Albergaria, J. T.; Delerue-Matos, C. Green production of zero-valent iron nanoparticles using tree leaf extracts. *Sci. Total Environ.* **2013**, *445–446*, 1–8.
- (20) Mohan Kumar, K.; Mandal, B. K.; Siva Kumar, K.; Sreedhara Reddy, P.; Sreedhar, B. Biobased green method to synthesize palladium and iron nanoparticles using *Terminalia chebula* aqueous extract. *Spectrochim. Acta, Part A* **2013**, *102*, 128–133.
- (21) Wang, T.; Jin, X.; Chen, Z.; Megharaj, M.; Naidu, R. Green synthesis of Fe nanoparticles using eucalyptus leaf extracts for

treatment of eutrophic wastewater. *Sci. Total Environ.* **2014**, 466–467, 210–213.

(22) Wang, Z.; Fang, C.; Megharaj, M. Characterization of iron–polyphenol nanoparticles synthesized by three plant extracts and their Fenton oxidation of azo dye. *ACS Sustain. Chem. Eng.* **2014**, 1–4.

(23) Tandon, P. K.; Shukla, R. C.; Singh, S. B. Removal of arsenic(III) from water with clay-supported zerovalent iron nanoparticles synthesized with the help of tea liquor. *Ind. Eng. Chem. Res.* **2013**, 52, 10052–10058.

(24) Machala, L.; Zboril, R.; Gedanken, A. Amorphous iron(III) oxide – A review. *J. Phys. Chem. B* **2007**, 111, 4003–4018.

(25) Machala, L.; Tuček, J.; Zbořil, R. Polymorphous transformations of nanometric iron(III) oxide: A review. *Chem. Mater.* **2011**, 23, 3255–3272.

(26) Marková, Z.; Machalová Šišková, K.; Filip, J.; Čuda, J.; Kolář, M.; Šafařová, K.; Medřík, I.; Zbořil, R. Air stable magnetic bimetallic Fe–Ag nanoparticles for advanced antimicrobial treatment and phosphorus removal. *Environ. Sci. Technol.* **2013**, 47, 5285–93.

(27) Filip, J.; Zboril, R.; Schneeweiss, O.; Zeman, J.; Cernik, M.; Kvapil, P.; Otyepka, M. Environmental applications of chemically pure natural ferrihydrite. *Environ. Sci. Technol.* **2007**, 41, 4367–4374.

(28) Hudson, R.; Hamasaka, G.; Osako, T.; Yamada, Y. M. A.; Li, C.-J.; Uozumi, Y.; Moores, A. Highly efficient iron(0) nanoparticle-catalyzed hydrogenation in water in flow. *Green Chem.* **2013**, 15, 2141–2148.

(29) Pechoušek, J.; Jančík, D.; Frydrych, J.; Navařík, J.; Novák, P. Setup of Mössbauer spectrometers at RCPTM. *AIP Conf. Proc.* **2012**, 1489, 186–193.

(30) Klencsár, Z.; Kuzmann, R.; Vértes, A. User-friendly software for Mössbauer spectrum analysis. *J. Radioanal. Nucl. Chem.* **1996**, 210, 105–118.

(31) Viollier, E.; Inglett, P. W.; Hunter, K.; Roychoudhury, A. N.; Van Cappellen, P. The ferrozine method revisited: Fe(II)/Fe(III) determination in natural waters. *Appl. Geochem.* **2000**, 15, 785–790.

(32) Staub, R. Research on physiology of nutrients of the planktonic cyanobacterium *Oscillatoria rubescens*. *Schweiz. Z. Hydrol.* **1961**, 23, 82–198.

(33) Gregor, J.; Jancula, D.; Marsálek, B. Growth assays with mixed cultures of cyanobacteria and algae assessed by in vivo fluorescence: One step closer to real ecosystems? *Chemosphere* **2008**, 70, 1873–1878.

(34) Bold, H. C. Torrey Botanical Society. *Bull. Torrey Bot. Club* **1949**, 76, 101–108.

(35) Water Quality – Determination of the inhibition of the mobility of *Daphnia magna* straus (Cladocera, Crustacea) – Acute toxicity test; ISO-6341; International Organization for Standardization (ISO): Geneva, Switzerland, 1996.

(36) Hoag, G. E.; Collins, J. B.; Holcomb, J. L.; Hoag, J. R.; Nadagouda, M. N.; Varma, R. S. Degradation of bromothymol blue by “greener” nano-scale zero-valent iron synthesized using tea polyphenols. *J. Mater. Chem.* **2009**, 19, 8671–8677.

(37) Takahashi, T.; Bassett, A. W. High-pressure polymorph of iron. *Science* **1964**, 145, 483–486.

(38) Marsalek, B.; Jancula, D.; Marsalkova, E.; Mashlan, M.; Safarova, K.; Tuček, J.; Zboril, R. Multimodal action and selective toxicity of zerovalent iron nanoparticles against cyanobacteria. *Environ. Sci. Technol.* **2012**, 46, 2316–2323.

(39) Auffan, M.; Achouak, W.; Rose, J.; Roncato, M.-A.; Chanéac, C.; Waite, D. T.; Masion, A.; Woicik, J. C.; Wiesner, M. R.; Bottero, J.-Y. Relation between the redox state of iron-based nanoparticles and their cytotoxicity toward *Escherichia coli*. *Environ. Sci. Technol.* **2008**, 42, 6730–6735.

(40) Papanikolaou, G.; Pantopoulos, K. Iron metabolism and toxicity. *Toxicol. Appl. Pharmacol.* **2005**, 202, 199–211.